

Original Article

The flavonoid TL-2-8 induces cell death and immature mitophagy in breast cancer cells via abrogating the function of the AHA1/Hsp90 complex

Hui-juan LIU¹, Xiao-xiao JIANG¹, Yi-zhen GUO¹, Fang-hui SUN¹, Xin-hui KOU¹, Yong BAO¹, Zhu-qing ZHANG¹, Zhao-hu LIN², Ting-bo DING¹, Lan JIANG³, Xin-sheng LEI⁴, Yong-hua YANG^{1,*}

¹Department of Pharmacology and Biochemistry, School of Pharmacy, Fudan University, Shanghai 201203, China; ²Chemical Biology, Roche Pharmaceutical Research and Early Development, Roche Innovation Center Shanghai, Shanghai 201203, China; ³Department of Biological Sciences, Oakland University, Rochester, MI 48309, USA; ⁴Department of Medicinal Chemistry, School of Pharmacy, Fudan University, Shanghai 201203, China

Abstract

The flavonoid quercetin exhibits significant anticancer activities with few side effects. In the current study, we characterized TL-2-8, a quercetin derivative, as a novel anticancer agent *in vitro* and *in vivo*. Cell proliferation and viability were assessed using Cell Counting Kit-8 and CellTiter-Blue assay, respectively. Cell death was examined using PI staining or a TUNEL assay. Mitophagy was determined by measuring autophagic flux and by confocal imaging. Protein expression was examined by Western blotting. We found that TL-2-8 selectively inhibited the proliferation and decreased the viability of various cancer cells (the anti-proliferation IC₅₀ values in MDA-MB-231, MDA-MB-468 and MCF-7 breast cancer cells at 72 h were 8.28, 8.56, and 9.58 μmol/L, respectively), and it displayed only slight cytotoxicity against normal MCF-10A and HEK-293 cells. In MDA-MB-231 and MDA-MB-468 breast cancer cells, TL-2-8 treatment induced the degradation of multiple Hsp90 client proteins without inducing Hsp70. TL-2-8 (3, 6, 12 μmol/L) dose-dependently inhibited the expression of AHA1, an activator of Hsp90 ATPase, and decreased Hsp90-AHA1 complex formation, leading to decreased Hsp90 chaperone function and reduced polo-like kinase 1 (PLK1) signaling. Consequently, impaired mitophagy was induced via the downregulation of lysosomal-associated membrane protein 2 (LAMP2). The *in vivo* anticancer effects of TL-2-8 were evaluated in an MDA-MB-231 breast cancer xenograft model, which was treated with TL-2-8 (25, 50, 100 mg·kg⁻¹·d⁻¹, *po*). Administration of TL-2-8 resulted in tumor growth inhibition rates of 37.9%, 58.9% and 70.9%, respectively, whereas quercetin treatment (100 mg·kg⁻¹·d⁻¹, *po*) produced only a lower tumor growth inhibition rate (49.5%). Furthermore, TL-2-8 treatment significantly extended the lifespan of mice bearing MDA-MB-231 breast cancer cell xenografts. Our results demonstrate that TL-2-8 induces significant cell death and immature mitophagy in breast cancer cells *in vitro* and *in vivo* via AHA1 abrogation.

Keywords: flavonoids; quercetin; breast cancer; heat shock proteins; AHA1 inhibitor; PLK1; mitophagy

Acta Pharmacologica Sinica (2017) 38: 1381–1393; doi: 10.1038/aps.2017.9; published online 1 May 2017

Introduction

Flavonoids have been exploited for their effectiveness and beneficial effects against various human cancers, as they have good antineoplastic activity and low toxicity^[1]. Quercetin, one of the most common flavonoids in the diet, is well known for its anti-carcinogenic potential. Recent studies have shown that quercetin has anti-proliferative effects, can induce cancer cell death via various cell signaling mechanisms and is able to

inhibit the enzymes responsible for the activation of carcinogens^[2–4]. Although some flavonoids affect the expression and activity of heat shock proteins (HSP)^[5], quercetin has no inhibitory effects on the expression of heat shock proteins including Hsp27, Hsp70 and Hsp90^[6,7].

Heat shock proteins are a family of proteins that are produced by cells in response to stressful conditions. The dramatic upregulation of heat shock proteins, which is known as the ‘heat shock response’, is primarily induced by heat shock factors (HSFs)^[8,9]. Heat shock protein 90 (Hsp90), a molecular chaperone, is responsible for the folding of numerous proteins into their mature and functional states. Therefore, Hsp90 is

*To whom correspondence should be addressed.
E-mail yonghuayang@hotmail.com
Received 2016-12-27 Accepted 2017-02-09

important in cancer development owing to its simultaneous regulation of various oncogenic proteins^[10]. A number of proteins in oncogenic pathways are Hsp90 client proteins, and many of these proteins are involved in cell proliferation, cell cycle progression and cell survival, which are crucial for tumor progression^[10,11]. Due to Hsp90 chaperoning, proteins that are crucial for tumor progression continue to operate rather than be degraded, thus supporting malignant transformation and cell cycle progression. Halting the chaperoning cycle is likely to achieve Hsp90 inhibition^[11]. Targeting Hsp90 with chemical inhibitors could induce the proteasomal degradation of Hsp90 client proteins, which could potentially lead to the disruption of multiple signaling pathways that are involved in carcinogenesis. Therefore, Hsp90 inhibition has been considered as a possible therapeutic strategy in cancers.

AHA1 has been suggested to function as a stimulator of the Hsp90 chaperone machinery. It is also a key co-chaperone of Hsp90 that is involved in the maturation, stabilization, activation and function of oncogenic proteins^[12]. Thus, disrupting the AHA1/Hsp90 complex would cause the depletion of client proteins and kinase clients that are involved in tumor cell proliferation and survival, as well as in all the hallmark traits of malignancy.

Autophagy is a stress-induced catabolic process in which substrates, including dysfunctional organelles, misfolded proteins and other macromolecules present in autophagosomes, are delivered to lysosomes for degradation. In mammalian cells, autophagy constitutes a multistep process that is coordinated by a wide range of molecular mechanisms in many cellular contexts and diseases, including cancer. The fusion of lysosomes with autophagosomes, which forms autolysosomes, is critical for autophagy-mediated degradation, which maintains cellular homeostasis in pathological conditions, including cancer^[13]. Mitophagy is the predominant mechanism used to remove superfluous and damaged mitochondria by autophagic degradation. Blocking autolysosome formation results in immature autophagy. Mitochondrial clearance upon Atg13 phosphorylation by Ulk1 kinase integrates mitophagy into the Hsp90-coordinated stress response, which controls mitochondrial homeostasis^[14]. The potential use of agents targeting autophagy in cancer prevention has attracted much attention. In the current study, we report that the flavonoid TL-2-8, a derivative of quercetin, impairs Hsp90-AHA1 complex formation through the inhibition of AHA1 expression, thus achieving effective antitumor activity both *in vitro* and *in vivo*. We also found that TL-2-8 abrogates the PLK1 (polo-like kinase 1) signaling pathway and LAMP2 expression, thus inhibiting mitophagy.

Materials and methods

Chemicals

The flavonoid TL-2-8 was synthesized by Dr Lei's laboratory (School of Pharmacy, Fudan University, Shanghai, China) and is also available from Shanghai Kanwin Biotechnology Co Shanghai, China). The structure of TL-2-8 was characterized, and the characterization data are as follows:

R_f 0.26 (petroleum ether/CH₂Cl₂/AcOEt 2/2/1), mp 115–117°C; ¹H NMR (400 MHz, CDCl₃) δ: 7.50–6.95 (m, 4H, Ar-H), 6.41 (s, 1H, Ar-H), 6.23–6.04 (m, 1H, CH₂CH=CH₂), 5.19–4.97 (m, 2H, CH=CH₂), 3.99 (s, 3H, OCH₃), 3.94 (s, 3H, OCH₃), 3.85 (s, 3H, OCH₃), 3.30 (d, *J*=4.3 Hz, 2H, Ar-CH₂-CH=CH₂), 2.82–2.62 (t, 2H, *J*=8.0 Hz, Ar-CH₂-CH₂), 1.64–1.49 (m, 1H, CH₂-CHMe₂), 1.47–1.32 (m, 2H, CH₂-CH₂-CH), and 0.91 (d, *J*=6.0 Hz, 6H, CHMe₂). ¹³C NMR (100 MHz, CDCl₃) δ: 177.8, 161.0, 160.9, 159.6, 159.1, 156.3, 136.9, 130.2, 125.8, 118.7, 115.1, 113.7, 110.7, 107.9, 91.2, 56.3, 55.8, 55.4, 38.6, 30.2, 28.4, 22.6, and 20.7. ESI-MS *m/z*: 423.2 [M+H]⁺. HRMS (ESI) calculated for C₂₆H₃₀O₅ [M+H]⁺ *m/z* as 423.2166 and found to be 423.2174.

Cell Lines, antibodies and reagents

MDA-MB-231, MDA-MB-468, MCF-7, BXP3, HCT116, MCF7-10A and HEK293 cells were all obtained from the American Tissue Culture Collection. MDA-MB-231 cells were maintained in RPMI-1640 containing 10% fetal bovine serum (FBS), while all of the other cells were maintained in DMEM containing 10% FBS.

The following antibodies were purchased from the indicated commercial sources: antibodies against Cdc37, cyclin D1, CDK1, CDK4, p-S326-HSF1, Hsp27, LAMP1 and LAMP2 were from Abcam (Cambridge, MA USA); the antibody against p62 was from Abnova (Taibei, Taiwan, China); the antibody against p53 was from BD Biosciences (Franklin Lakes, NJ USA); the antibodies against AKT, p-AKT, HOP, LC3, NBR1, NDP52, Parkin, Pink1, PLK1, p-T210-PLK1 and Vps34 were from Cell Signaling Technology (Beverly, MA USA); the antibodies against Hsp40, Hsp70, Hsp90α and P23 were from Enzo Life Sciences (Shanghai, China); the antibodies against AHA1, HSF1 and Tom20 were from Santa Cruz Biotechnology (Dallas, TX, USA); the antibodies against FLAG, M2 agarose and β-actin were from Sigma (Shanghai, China); and the antibody against p-Ser378-Parkin was from Thermo Fisher Scientific (Waltham, MA USA). All of the secondary antibodies were purchased from Jackson Immuno Research (West Grove, PA, USA).

The plasmid expressing FLAG (F)-hsp90 has previously been described^[12].

Cell proliferation, viability and half-maximal inhibitory concentration

Cell proliferation was determined by the cell counting method using Cell Counting Kit-8 (CCK-8, Dojindo Laboratories), and cell viability was assessed using the CellTiter-Blue® Assay (Promega), according to the manufacturers' protocols. Briefly, 1.5×10³ cells were seeded in each well of a 96-well plate in triplicate and incubated for 24 h prior to treatment with different concentrations of TL-2-8 for 72 h. After treatment, 10 μL of the CCK-8 or Cell Viability Assay solution was added to each well in the plate, followed by incubation for 2 h. The absorbance was measured at an excitation of 450 nm or 560 nm and an emission of 590 nm using a microplate reader. The cell viability was calculated using the data obtained from the wells that contained known numbers of viable cells. The 50% inhibitory concentration (IC₅₀) was calculated and presented as

a weighted regression plot.

Western blot analyses

Cellular extracts were prepared by directly adding lysis buffer containing 10 mmol/L Tris-HCl (pH 8.8), 150 mmol/L NaCl, 1 mmol/L EDTA, 1% *w/v* NP-40, 0.1% *w/v* SDS, 1 mmol/L phenylmethylsulfonyl fluoride (PMSF) and 1 mmol/L protease inhibitor (Roche) to the cells on ice. In the *in vivo* study, the tumor tissue samples were homogenized for tissue lysate extraction. Both the cell and tissue lysates were centrifuged, and the supernatants were collected. The protein concentration in the cell lysates was quantified using the Quick Start Bradford Dye Reagent (Bio-Rad), and the samples were subjected to SDS-PAGE. Western blot analysis was performed as described previously^[12]. β -Actin was used as a loading control.

PI staining for the cell death assay

MDA-MB-231 cells were cultured in glass-bottomed dishes in RPMI-1640 medium containing 10% FBS in the presence or absence of specific concentrations of TL-2-8; MDA-MB-468 cells were treated the same way and cultured in DMEM containing 10% FBS. After a 24 h incubation, the cells were incubated with 10 μ g/mL PI at 37°C for 15–30 min in the dark. The cells were counterstained using Vectashield mountant containing 4', 6-diamidino-2-phenylindole (DAPI) for 5 min at 37°C and imaged using a Zeiss LSM510 confocal microscope with a 20 \times objective.

Transfections, immunoprecipitation assays, and immunoblots

Following culture in the plates for 24 h, MDA-MB-231 and MDA-MB-468 cells were transfected with Lipofectamine 2000 according to the protocol provided by Invitrogen (Carlsbad, CA, USA). Transfected cells were cultured for 24 h in full medium containing TL-2-8 or vehicle. Cellular extracts were prepared by directly adding lysis buffer to the cells on ice. For the immunoprecipitation (IP) assays, the cellular extracts were prepared, and IP was performed as described previously^[12]. For immunoblotting, cellular extracts or immunoprecipitates were separated by SDS-PAGE, transferred to a nitrocellulose membrane, probed with antibodies, and visualized with enhanced chemiluminescence, as described previously^[12].

Confocal microscopy for mitophagy detection

MDA-MB-231 cells were cultured on a chamber slide for 18 h in RPMI-1640 medium containing 10% FBS in the presence or absence of 12 μ mol/L TL-2-8 and stained with antibodies against Parkin and Tom20. Briefly, after an 18-h incubation, the cells were washed with 1 \times PBS and fixed with 4% paraformaldehyde for 10 min. After this, the slides were blocked with 3% bovine serum albumin (BSA) for 30 min and incubated with the primary antibody at a dilution of 1:100 in BSA for 4 h. After three washes with PBS, the slides were incubated with DyLight 549 goat anti-rat (H+L) IgG and FITC goat anti-rabbit (H+L) IgG secondary antibodies for 1 h at a 1:500 dilutions. After three more washes with PBS, the cells

were counterstained using Vectashield mountant containing DAPI and imaged using a Zeiss LSM510 confocal microscope with a 63 \times objective.

Live cell imaging with fluorescent tracers

Intracellular acidic compartments were labeled by incubating live cells with LysoTracker Deep Red (Invitrogen) added to DMEM to a final concentration of 1 μ mol/L for 3 h at 37°C. For labeling with dextran AF-488, the cells were washed twice with DMEM containing 10% FBS followed by incubation with 0.5 mg/mL dextran AF-488 in the same medium for 4 h at 37°C. Then, the cells were washed three times in tracer-free DMEM containing 10% FBS. Phase-contrast and fluorescent images of the living cells were acquired using a Zeiss LSM510 microscope.

Stable MDA-MB-231_LAMP2-expressing cells and confocal microscopy

cDNA encoding LAMP2 was sub-cloned into the pcDNA3-flag vector and then transfected into MDA-MB-231 cells. Then, 5 μ g/mL of puromycin (Invitrogen) was used to select for stable flag-LAMP2-expressing cells, which are referred to here as MDA-MB-231_LAMP2 cells. MDA-MB-231_LAMP2 and MDA-MB-231 cells were infected with lentivirus encoding tf-LC3^[13], followed by treatment with 12 μ mol/L TL-2-8 for 18 h. Images were acquired with an LSM710 confocal microscope with a 63 \times objective (Carl Zeiss).

MDA-MB-231 breast cancer xenograft model

To determine the *in vivo* antitumor efficacy of TL-2-8, MDA-MB-231 breast cancer xenografts were established in nude mice. The use and care of the experimental animals were approved by the Institutional Animal Care and Use Committee (IACUC), Roche R & D Center (Shanghai, China). Briefly, MDA-MB-231 cells in log-phase growth were trypsinized and washed twice with PBS. 0.2 mL of PBS containing 1 \times 10⁷ cells was injected under aseptic conditions into the mammary fat pads of four-week-old female BALB/c nude mice. When the average tumor volume reached approximately 100 mm³, the mice were randomized into five groups (six mice per group).

TL-2-8 was dissolved in saline solution containing 5% DMSO. The tumor volume and the animals' body weight were measured once per week. Tumor tissue was collected for histological, immunohistochemical and Western blot analysis. Doses of TL-2-8 (0, 25, 50, and 100 mg/kg) and quercetin (100 mg/kg) were administered orally once daily. Tumor volumes and body weight were measured once per week, and clinical symptoms were observed every day. The tumor size was calculated according to the following formula: tumor volume (mm³)=0.52 \times L \times W², where L is the length and W is the width. Treatments producing >20% net body weight loss were considered toxic.

TUNEL assay

Apoptotic cells in the MDA-MB-231 xenograft tumors were identified by terminal deoxynucleotidyl transferase-mediated

dUTP nick end-labeling (TUNEL) staining using the *In Situ* Cell Death Detection Kit (Roche) according to the manufacturer's protocol. Briefly, the tissue sections were deparaffinized before rehydration with decreasing concentrations of ethanol. After washing with 0.85% NaCl and PBS, the tissue sections were fixed with 4% formaldehyde for 15 min. Following washing with PBS, the tissue sections were covered with proteinase K solution for 15–20 min. After another PBS wash, the tissue sections were covered with the TUNEL reaction mixture and incubated for 1 h in the dark. DAPI counterstaining was followed by a final PBS wash, and tissue sections were then examined and photographed using fluorescence microscopy (Zeiss). The average number of fluorescent dots in three images from each treatment group was calculated.

Statistical analysis

Data are presented as the mean \pm SEM and were analyzed using the Graphpad software (USA). Differences between the means of the groups were determined using one-way ANOVA. $P < 0.05$ was considered to indicate a statistically significant difference.

Results

The flavonoid TL-2-8 induced breast cancer cell death

Quercetin modulates a number of important proteins in cellular signal transduction pathways that are linked to processes involved in cell death and cell survival or cell proliferation^[15]. We synthesized the flavonoid TL-2-8 (Figure 1A) and investigated its effects on the proliferation of breast cancer cells. Different TL-2-8 concentrations were applied to MDA-MB-231, MDA-MB-468 and MCF-7 breast cancer cells for 72 h. The assessment of the effect of TL-2-8 on cell proliferation was performed using Cell Counting kit-8 (CCK-8), and cell viability was assessed using the CellTiter-Blue assay. As shown in Figure 1B, TL-2-8 dose-dependently inhibited cell proliferation, and the IC₅₀ values at 72 h were 8.28, 8.56, and 9.58 $\mu\text{mol/L}$, in the MDA-MB-231, MDA-MB-468 and MCF-7 breast cancer cell lines, respectively. TL-2-8 also reduced the viability of MDA-MB-231, MDA-MB-468 and MCF-7 breast cancer cells with IC₅₀ values of 7.94, 8.96, and 9.45 $\mu\text{mol/L}$, respectively (Figure 1C). TL-2-8 reduced breast cancer cell viability in a dose-dependent manner.

To investigate the impact of TL-2-8 on other cancer cell lines, the effects of TL-2-8 on cell proliferation and viability were tested in BXP3 pancreatic cancer cells and HCT116 colon cancer cells. BXP3 and HCT116 cells were more sensitive to TL-2-8 than were breast cancer cells, with proliferation IC₅₀ values of 3.29 and 5.89 $\mu\text{mol/L}$, respectively, and viability IC₅₀ values of 3.15 and 5.75 $\mu\text{mol/L}$, respectively (Figure S1-A and S1-B). Strikingly, TL-2-8 exhibited only slight cell toxicity, with IC₅₀ values of 35.89 and 50.8 $\mu\text{mol/L}$ in normal MCF-10A and HEK-293 cells, respectively (Figure S1-A and S1-B). Therefore, TL-2-8 is selectively cytotoxic for cancer cells versus normal cells.

Propidium iodide (PI) is membrane impermeable and generally excluded from viable cells. Thus, it is commonly used

for dead cell identification. Therefore, PI was used to identify the number of dead cells after TL-2-8 treatment. As shown in Figures 1D and 1E, TL-2-8 markedly induced breast cancer cell death in a dose-dependent manner; DMSO was used as a vehicle control (CTL). However, the mechanism by which TL-2-8 induced cell death still needed to be elucidated.

TL-2-8 decreased the expression of Hsp90 co-chaperones in breast cancer cells

Aside from its ATPase activity, Hsp90 chaperone function requires conformational transformation, which is achieved by the formation of an integrated complex by a series of co-chaperones^[10, 11]. Important co-chaperones include Hsp70, Hsp40, Hsp27, HOP, P23, Cdc37 and AHA1, the latter of which is specific for oncoprotein kinases. Inhibitors of Hsp90 usually target the N-terminal domain at the ATP-binding site. Some ATP-binding site inhibitors of Hsp90 that are in clinical trials, such as 17-AAG, PU-H71 and NVP-AUY922, have been well studied. Recently, however, these inhibitors were found to confer cancer cell resistance owing to the strong transcriptional induction of the heat shock response, which increases the cellular levels of pro-survival chaperones such as Hsp27 and Hsp70^[16].

To investigate whether the flavonoid TL-2-8 could affect the expression of Hsp90 co-chaperones, MDA-MB-231 and MDA-MB-468 breast cancer cells were selected for further study by Western blotting. After treating cells with increasing concentrations of TL-2-8 for 24 h, no obvious changes were observed in the expression levels of several co-chaperones including Cdc37, HOP and P23. However, a dramatic reduction in AHA1 expression was observed in these breast cancer cells (Figures 2A and 2B). In contrast to other classic Hsp90 inhibitors, the flavonoid TL-2-8 did not lead to the transcriptional induction of the heat shock response. The expression of the heat shock proteins Hsp90, Hsp70, Hsp40 and Hsp27 was not induced; instead, the expression of some of these proteins was inhibited (Figures 2C and 2D). These results showed that TL-2-8 affected the biological function of Hsp90, and compared with other Hsp90 inhibitors that activate the expression of heat shock proteins to induce drug resistance in tumors, TL-2-8 may not induce drug resistance in cancer therapy.

TL-2-8 induced the degradation of Hsp90 client proteins in breast cancer cells

To verify that TL-2-8 is an Hsp90 inhibitor, we tested whether TL-2-8 could induce the degradation of Hsp90 client proteins in MDA-MB-231 and MDA-MB-468 breast cancer cells by treating these cells with increasing concentrations of TL-2-8. As shown in Figures 3A and 3B, TL-2-8 treatment resulted in the downregulation of the Hsp90 client proteins p-Akt, CDK1, CDK4, cyclin D1 and p53 in a concentration-dependent manner. More importantly, treatment with TL-2-8 also resulted in the progressive downregulation of the expression of PLK1 and HSF1, as well as the levels of the active forms T210-phosphorylated PLK1 and S326-phosphorylated HSF1 (Figures 3C and 3D). PLK1 and HSF1 are both Hsp90 cli-

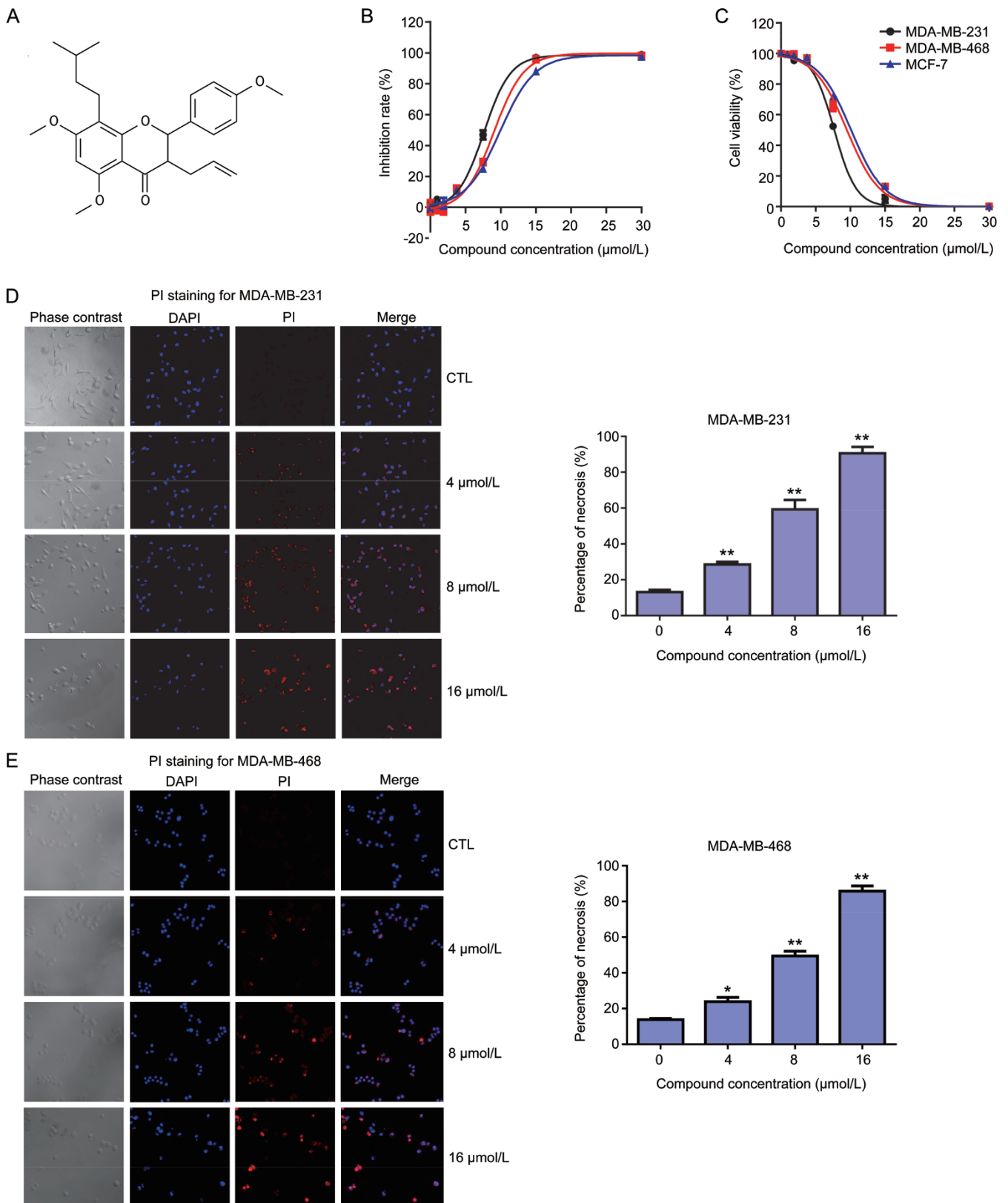


Figure 1. TL-2-8 induced breast cancer cell death. (A) Chemical structure of TL-2-8. Inhibition of cell proliferation (B) and cell viability (C) were tested on indicated cells treated with increasing concentrations of TL-2-8 for 72 h. Cell death were tested on breast cancer MDA-MB-231 (D) and MDA-MB-468 (E) cells treated with the indicated concentrations of TL-2-8 for 24 h, DMSO was used as vehicle control (CTL). Cell death was presented as the percentage of viable cells compared to the control cells, and the representative images were from three independent experiments. Original magnification: 20 \times . Student's *t*-test. Mean \pm SEM. **P*<0.05, ***P*<0.01.

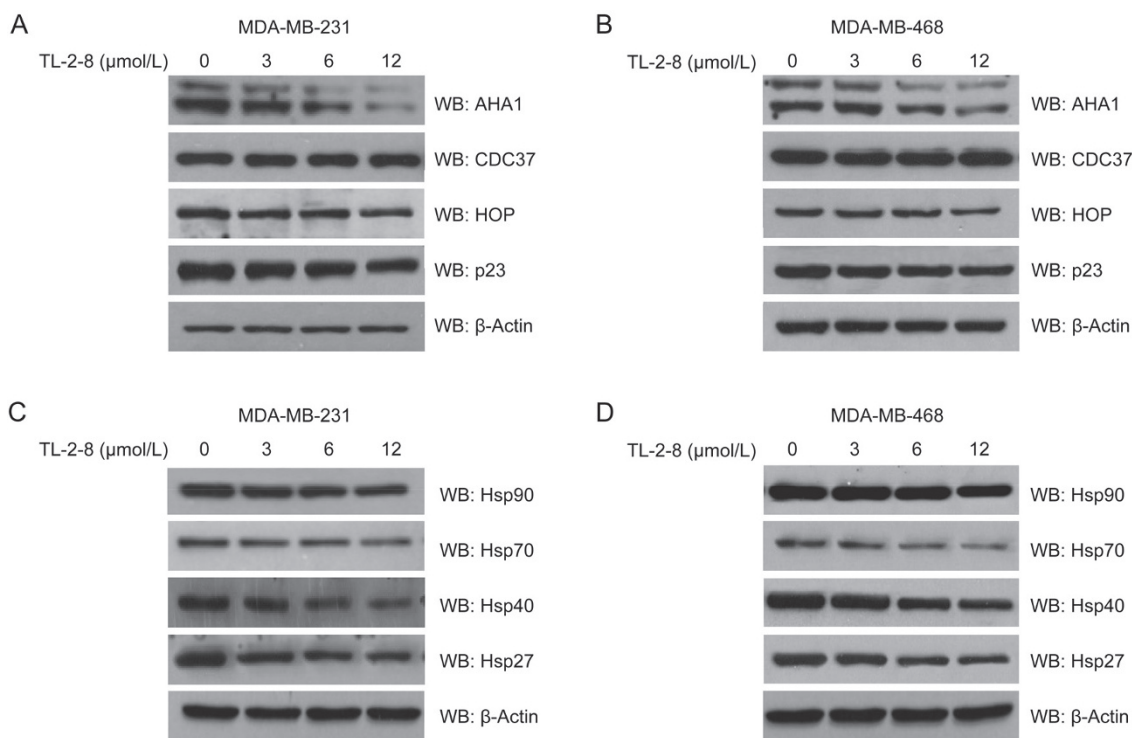


Figure 2. Effect of TL-2-8 on the expression of Hsp90 co-chaperones in breast cancer cells. The expression of Hsp90 co-chaperones was detected in MDA-MB-231 (A) and MDA-MB-468 (B) cells treated as indicated for 24 h. The expression of heat shock proteins was also detected in TL-2-8-treated MDA-MB-231 (C) and MDA-MB-468 (D) cells. β-Actin was used as loading control.

ent proteins; PLK1 and HSF1 are also the signaling proteins upstream of heat shock proteins. This negative feedback role makes the antitumor effects of TL-2-8 more significant. As TL-2-8 decreased the expression of Hsp90 client proteins, we tested whether the decrease in cyclin D1 levels in the presence of TL-2-8 was due to protein destabilization. MDA-MB-231 and MDA-MB-468 cells were incubated with either TL-2-8 or DMSO in the presence of cycloheximide (CHX, an inhibitor of protein synthesis) for 6, 12 and 24 h, and the protein levels of cyclin D1 and β-actin were measured. As shown in Figures 3E and 3F, TL-2-8 treatment decreased cyclin D1 levels, whereas CHX treatment had no effect, suggesting that the depletion of cyclin D1 by TL-2-8 was due to enhanced instability. These data supported a specific effect of TL-2-8 on the stability of the cyclin D1 protein, and indicate that TL-2-8 also induces Hsp90 client protein degradation in breast cancer cells.

AHA1 was critical for the TL-2-8-induced downregulation of Hsp90 client proteins in breast cancer cells

The above results indicated that TL-2-8 has the characteristics of an Hsp90 inhibitor. It is well known that the function of Hsp90 is dependent on its ATPase activity, which is activated by AHA1. AHA1 plays a significant role in the ATP-driven Hsp90 chaperone cycle owing to its interaction with Hsp90. As the Hsp90/AHA1 complex regulates downstream kinase client maturation and activity^[17], abrogation of the Hsp90/AHA1 complex may lead to a reduction in the activity of various kinases.

As shown in Figure 4, a progressive decline in AHA1 expression was observed in MDA-MB-231 cells expressing ectopic (Figure 4A) or endogenous (Figure 4C) Hsp90 after treatment with increasing amounts of TL-2-8. Similar results were also observed in MDA-MB-468 cells expressing ectopic (Figure 4B) or endogenous Hsp90 (Figure 4D). Subsequently, we showed that the flavonoid TL-2-8 decreased Hsp90/AHA1 complex formation in MDA-MB-231 cells and MDA-MB-468 cells. To confirm that AHA1 is the key element for the stabilization of Hsp90 client proteins, AHA1 was ectopically expressed in MDA-MB-231 and MDA-MB-468 cells, and cells were then treated with TL-2-8. As shown in Figure 4E, the expression levels of PLK1, HSF1, CDK1 and cyclin D1 were partially rescued by ectopic expression of AHA1. These data demonstrate that the flavonoid TL-2-8 is an AHA1 inhibitor that diminishes Hsp90/AHA1 complex formation.

TL-2-8-induced immature mitophagy

Mitophagy is controlled by the serine/threonine kinase Pink1 (PTEN-induced putative kinase 1) and the E3 ligase Parkin1, both of which are necessary for directing damaged mitochondria for mitophagy to keep cells healthy^[18, 19]. Mitochondrial depolarization inactivates protein transport into the mitochondria and proteasomal degradation, which leads to the accumulation of Pink1 on the outer membrane of mitochondria and results in the recruitment of Parkin from the cytosol to damaged mitochondria. Pink1 phosphorylates the ubiquitin-like domain of Parkin at serine 65 to activate its E3 ligase

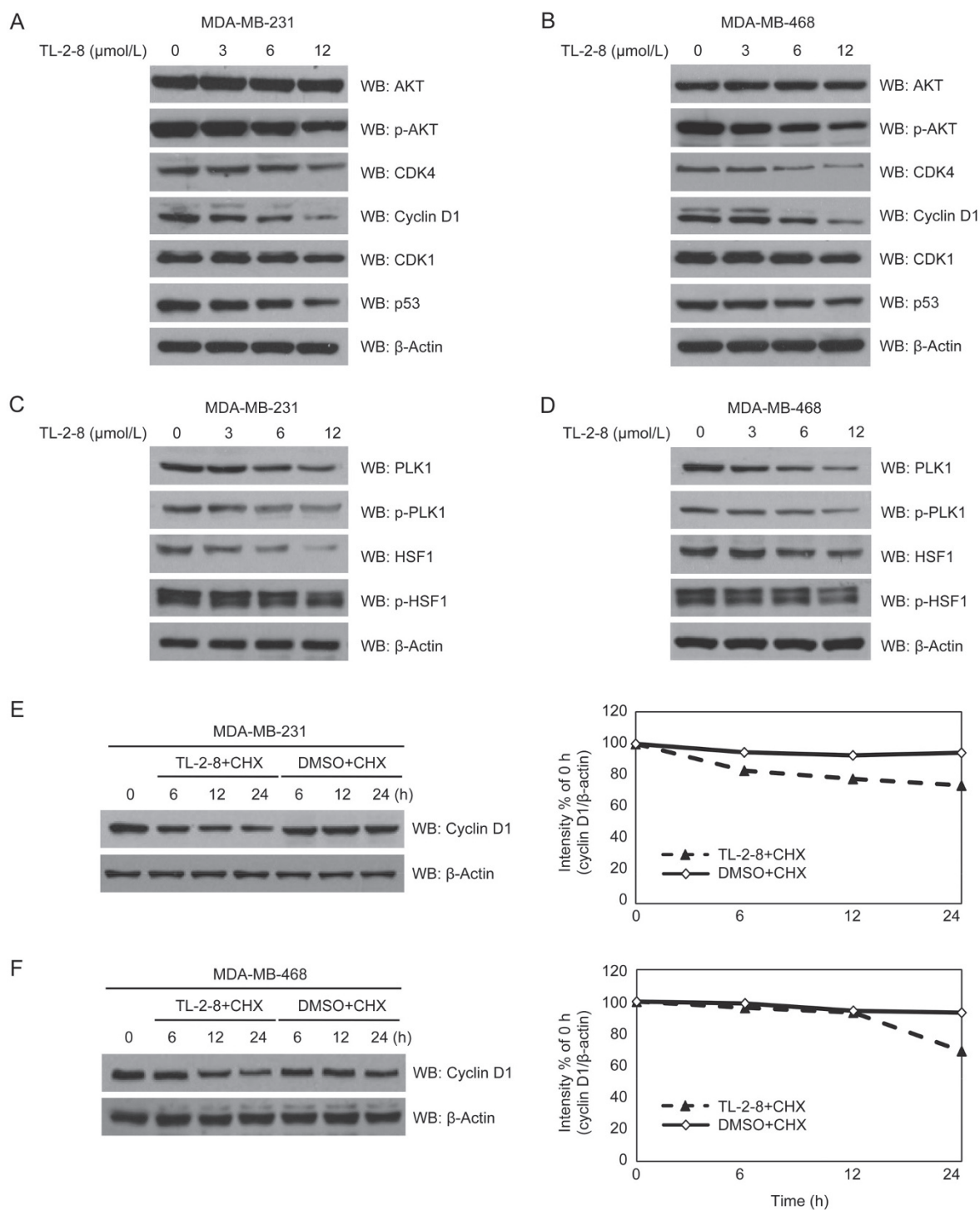


Figure 3. Effect of TL-2-8 on the expression of Hsp90 client proteins in breast cancer cells. The expression of Hsp90 client proteins were detected in MDA-MB-231 (A) and MDA-MB-468 (B) cells treated with the indicated concentrations of TL-2-8 for 24 h. The expression levels of PLK1 and HSF1 and their active forms were detected in MDA-MB-231 (C) and MDA-MB-468 (D) cells treated as above. MDA-MB-231 (E) and MDA-MB-468 (F) cells were incubated with 50 μmol/L CHX in the presence of DMSO or 6 μmol/L TL-2-8 for the indicated hours followed by Western blotting for the detection of cyclin D1. β-Actin was used as loading control.

activity, which is involved in mitophagy^[20, 21]. Recently, PLK1 was reported to interact with the C-terminal region of Parkin and phosphorylate S378, which results in a dramatic enhancement of its E3 ligase activity^[22]. This prompted us to explore

whether mitophagy was regulated by a TL-2-8-induced disturbance of the Parkin protein.

To analyze the effects of TL-2-8 on autophagy, the expression levels of autophagy-related proteins in TL-2-8-treated

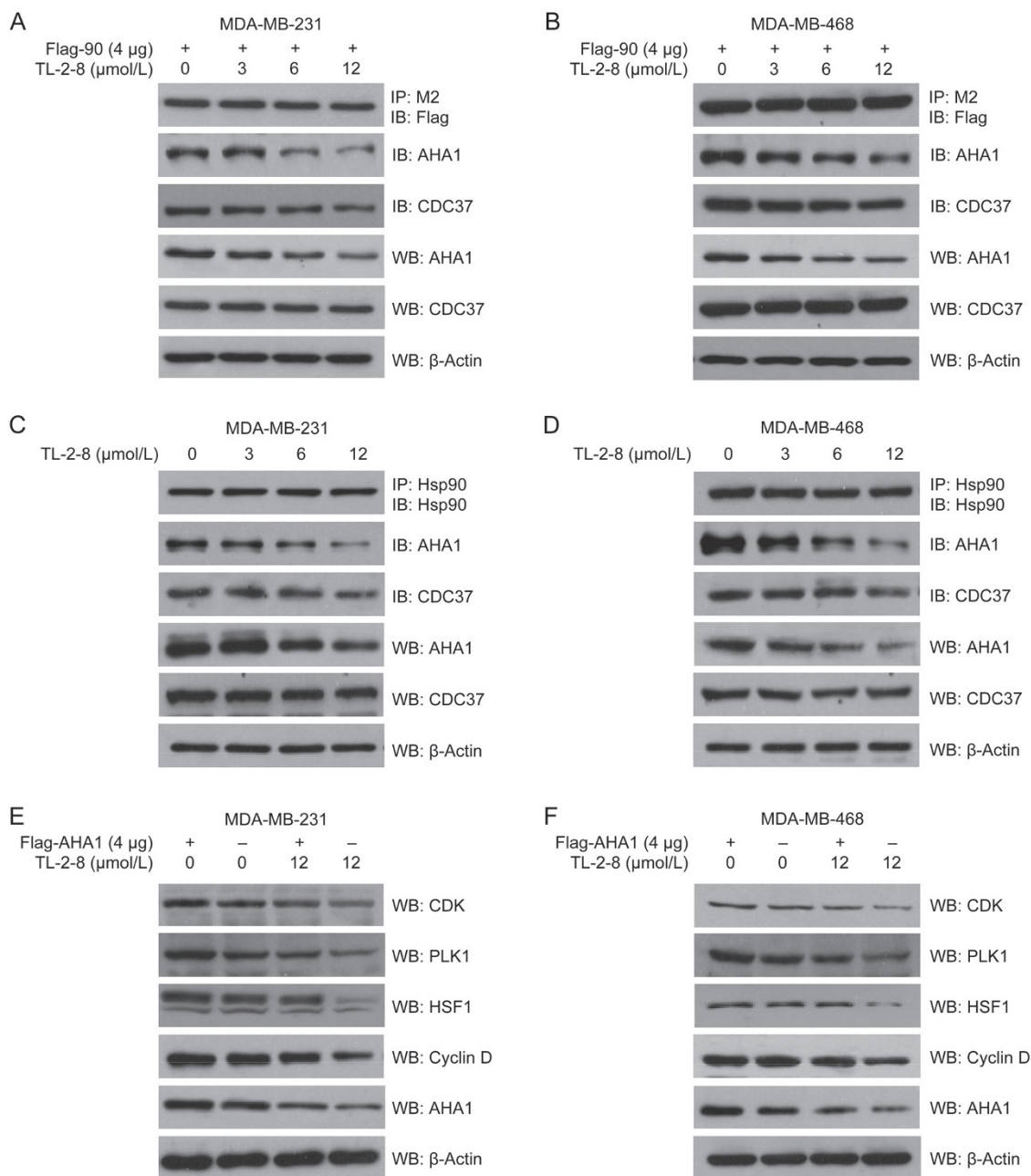


Figure 4. AHA1 is critical for TL-2-8 downregulation of Hsp90 client proteins in breast cancer cells. Ectopically expressed Hsp90 formed complexes with endogenous AHA1. These complexes were decreased in TL-2-8 treated MDA-MB-231 (A) and MDA-MB-468 (B) cells. Cells transfected with flag-Hsp90α (4 μg) were treated with the indicated concentrations of TL-2-8 for 24 h. Cell lysates were immunoprecipitated with M2 beads followed by immunoblotting with AHA-1 or anti-rabbit FLAG antibody. Endogenous Hsp90 formed complexes with endogenous AHA1; these were decreased in MDA-MB-231 (C) and MDA-MB-468 (D) cells treated with the indicated concentrations of TL-2-8. After 24 h, the cell lysates were immunoprecipitated with protein A/G beads and anti-Hsp90 antibody, followed by immunoblotting with anti-AHA1 antibody or anti-Hsp90 antibody. AHA1 overexpression rescued the expression of Hsp90 client proteins in breast cancer MDA-MB-231 (E) and MDA-MB-468 (F) cells treated as indicated. β-Actin was used as loading control.

breast cancer cells were investigated by Western blotting. We found that intracellular levels of LC3-II were increased by TL-2-8 treatment (Figures 5A and 5B). Consistent with the expression of LC3-II, the expression of Pink1 and Parkin was also significantly and dose-dependently increased by TL-2-8 treatment. Nevertheless, Tom20, a receptor protein on the mitochondrial outer membrane, was not degraded upon Pink1

and Parkin induction. Among the autophagy adaptor proteins, the degradation of neither p62 nor NDP52 was observed upon TL-2-8 treatment (Figures 5A and 5B). In contrast, NBR1 levels were elevated in response to TL-2-8 treatment. To confirm the induction of mitophagy, MDA-MB-231 cells treated with TL-2-8 for 18 h were stained with antibodies against Parkin (green) and Tom20 (red), and this revealed that the colocal-

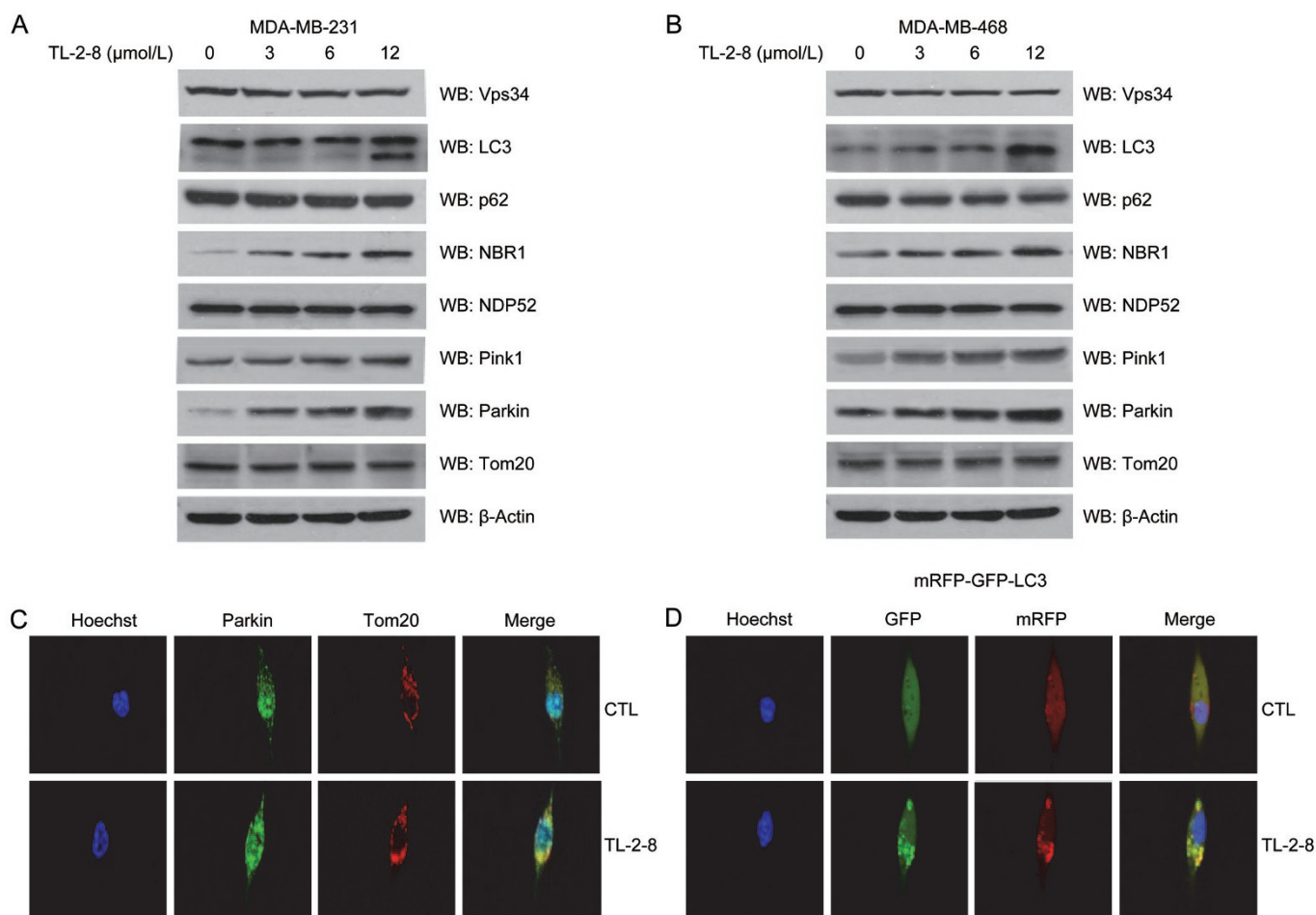


Figure 5. TL-2-8 induced immature mitophagy. Autophagy-related proteins were detected by Western blotting in breast cancer MDA-MB-231 (A) and MDA-MB-468 (B) cells treated with the indicated concentrations of TL-2-8 for 24 h. β -Actin was used as loading control. (C) Recruitment of Parkin to damaged mitochondria was detected by immunostaining with antibodies against Tom20 (red) and Parkin (green) in MDA-MB-231 cells treated with the vehicle or 12 μ mol/L TL-2-8 for 18 h. (D) Autophagy was detected in MDA-MB-231 cells infected with lentivirus encoding tf-LC3 for 48 h, followed by treatment with the vehicle or 12 μ mol/L TL-2-8 for 18 h. The nuclei were stained with DAPI and representative fluorescence images are shown.

ization of Parkin and aggregated mitochondria (Tom20) was increased relative to the levels observed in the vehicle control (CTL) (Figure 5C). These results indicated that mitochondrial damage occurred upon TL-2-8 treatment and that Parkin was selectively recruited to the damaged mitochondria.

As shown in Figure 5A, TL-2-8 induced a moderate increase in the expression of LC3-II. Hence, the distribution of mRFP-GFP-LC3 (tf-LC3) was examined following TL-2-8-mediated induction of both Pink1 and Parkin expression. GFP loses its fluorescence in the acidic environment of lysosomes, while mRFP maintains its fluorescence. Thus, green puncta merged with red ones yield yellow dots that are indicators of autophagosomes. In contrast, the red puncta in merged images are indicative of autolysosomes^[13]. As Figure 5D illustrates, the numbers of green and red puncta were both dramatically increased after TL-2-8 treatment compared with vehicle treatment (CTL). However, only the number of yellow puncta was significantly increased in the merged images, indicating increased autophagosome formation but not increased for-

mation of mature autolysosomes. These results suggested that TL-2-8 treatment induced autophagosome formation but prevented the maturation of autolysosomes. Consistent with this, TL-2-8-dependent accumulation of NBR1 (Figures 5A and 5B) also indicated the blockade of autophagosome-lysosome fusion.

LAMP2 was crucial for TL-2-8-induced defective mitophagy

To verify the TL-2-8-mediated blockade of autolysosomal maturation, a 3-h incubation with a fluorescent acidotropic LysoTracker dye, which specifically stains cellular lysosomes, resulted in red fluorescent staining of the lysosomal compartments present within MDA-MB-231 cells. This was followed by staining with dextran-Alexa Flour 488 for 4 h to determine if the dextran-labeled endosomal compartments would merge with the LysoTracker dye-labeled lysosomes. As shown in Figure 6A, the transportation of endocytosed dextran from endosomes to lysosomes for degradation was significantly inhibited by TL-2-8 treatment compared with vehicle treatment (CTL).

This clearly indicated that TL-2-8 blocks autophagosome-lysosome fusion.

Next, we investigated the key proteins related to autophagosome and lysosome fusion. LAMP2 is one of the proteins required for the proper fusion of a lysosome with autophagosomes^[23]. LAMP2 depletion impairs autolysosome formation, leading to the accumulation of autophagic vacuoles and the severe impairment of autophagic degradation^[24, 25]. As shown in Figure 6B, we found that LAMP2 expression, but not Lamp1 expression, was significantly decreased following cell treatment with increasing amounts of TL-2-8. However, TL-2-8 treatment did not cause a dramatic reduction in the expression of Rab7, which is responsible for endosome maturation, endosome transportation, and the fusion of endosomes with lysosomes. According to these results, we propose that TL-2-8 blocks autophagosome-lysosome fusion by reducing LAMP2 expression. To further confirm this point, we showed that TL-2-8 induced significantly more red puncta in MDA-MB-231_LAMP2 cells than in MDA-MB-231 cells (Figure 6C). LAMP2 overexpression improved the maturation of TL-2-8-induced autophagy. This was shown by the degradation of p62 in MDA-MB-231_LAMP2 cells but not in parental MDA-MB-231 cells (Figure 6D). Therefore, TL-2-8 promotes

mitochondrial impairment, leading to the accumulation of dysfunctional mitochondria and thus to cellular degeneration.

TL-2-8 inhibited tumor growth in an MDA-MB-231 breast cancer xenograft model

After confirming that TL-2-8 reduced cell viability and inhibited cell growth *in vitro*, we examined whether TL-2-8 could inhibit tumor growth in a xenograft model of breast cancer. To evaluate TL-2-8 as an anti-cancer therapeutic agent for breast cancer and compare it with quercetin, a bioflavonoid with cancer-preventing properties, an MDA-MB-231 breast cancer cell line was used to create a mouse subcutaneous tumor model. As expected, oral administration of TL-2-8 elicited a strong antitumor effect and significantly suppressed tumor growth compared to treatment with quercetin or the vehicle control. The tumor growth inhibition rates at three doses (25, 50, and 100 mg/kg) were 37.9%, 58.9% and 70.9%, respectively. Strikingly, TL-2-8 exerted a better *in vivo* anti-cancer effect than did quercetin (49.5%) at the same dosage (100 mg/kg) (Figure 7A). Similarly, to the induction of cell death *in vitro* (Figure 1), analysis of the TL-2-8-mediated induction of breast cancer cell death *in vivo* was performed using a TUNEL assay. We found that TL-2-8 caused direct cell death in breast cancer cells *in*

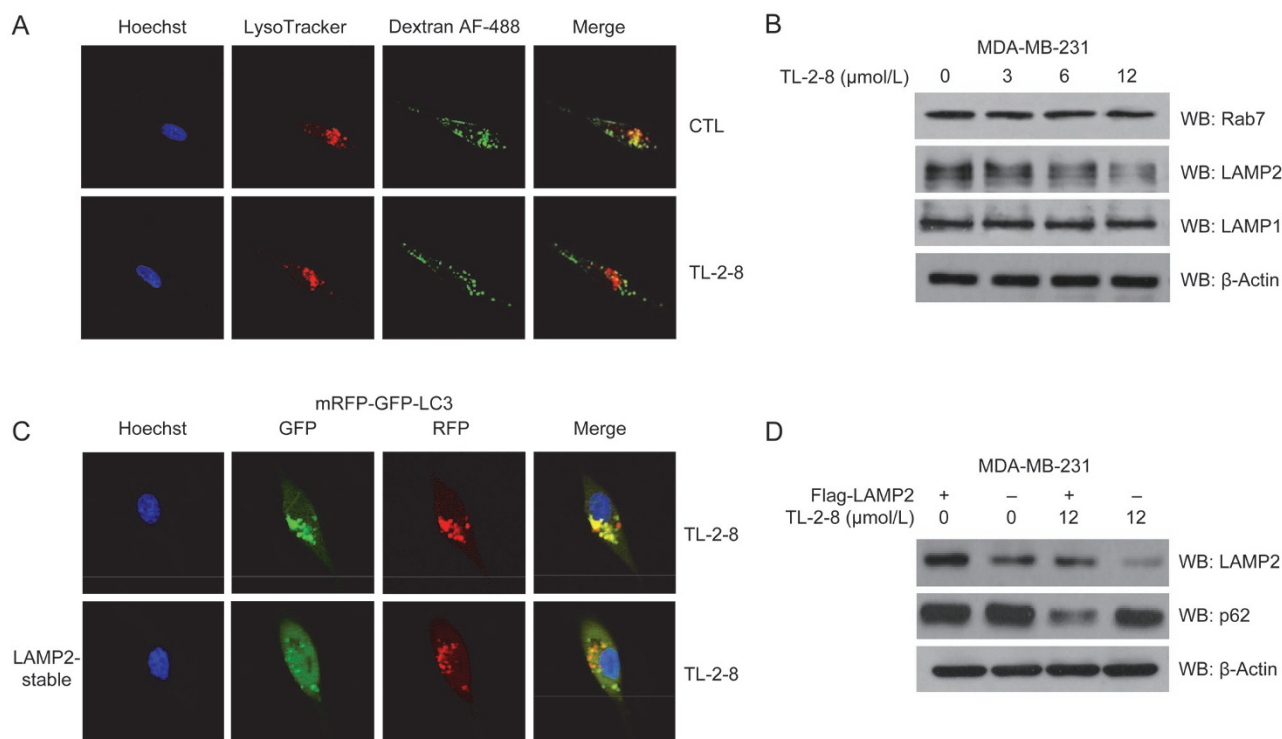


Figure 6. LAMP2 is critical for the maturation of TL-2-8-induced mitophagy. (A) Endosome-lysosome fusion was detected in MDA-MB-231 cells treated with the vehicle or 12 $\mu\text{mol/L}$ TL-2-8 for 18 h followed by incubation with LysoTracker Red (red) for 3 h and dextran AF-488 (green) for another 4 h. The nuclei were stained with DAPI. Representative fluorescence images merged with DIC images are shown. (B) Proteins associated with the autolysosome were detected in MDA-MB-231 cells treated with increasing concentrations of TL-2-8 for 18 h. (C) Autophagy was detected in MDA-MB-231 cells harboring control vector or vector expressing LAMP2 infected with lentivirus encoding tf-LC3 for 48 h, followed by treatment with 12 $\mu\text{mol/L}$ TL-2-8 for 18 h. The nuclei were stained with DAPI and representative fluorescence images are shown. (D) MDA-MB-231 cells harboring control vector or vector expressing LAMP2 were treated with or without 12 $\mu\text{mol/L}$ TL-2-8 for 18 h, followed by Western blotting for the detection of LAMP2 and p62. β -Actin served as loading control.

in vivo (Figure 7B). More importantly, no visible adverse effects of TL-2-8 were observed, as there was no dramatic reduction in the body weight of mice treated with TL-2-8 compared with those treated with vehicle control (Figure S1-C).

Next, we examined the longevity of the post-xenograft mice as an indicator of the tumorigenicity of the MDA-MB-231 cells. The median survival time for each group of mice was calculated and is shown in Figure S2. A Kaplan-Meier plot (Figure S2), in which each arm represents the percentage of animals alive at the indicated time point following treatment, illustrates that TL-2-8 significantly prolonged the survival of MDA-MB-231 tumor-bearing mice. Moreover, we tested

the expression levels of proteins associated with Hsp90 and mitophagy in the tumor samples. The expression patterns in the tumor tissue (Figures 7C and 7D) were consistent with the expression patterns observed *in vitro* upon TL-2-8 treatment (Figures 2C, 2D and Figures 5A, 5B). These results strongly suggested that the antitumor activity of TL-2-8 is attributed to the inhibition of AHA1 accompanied by the impairment of LAMP2-dependent mitophagy.

Discussion

Hsp90 is an essential ATPase-dependent molecular chaperone that is abundantly and ubiquitously expressed in eukaryotic

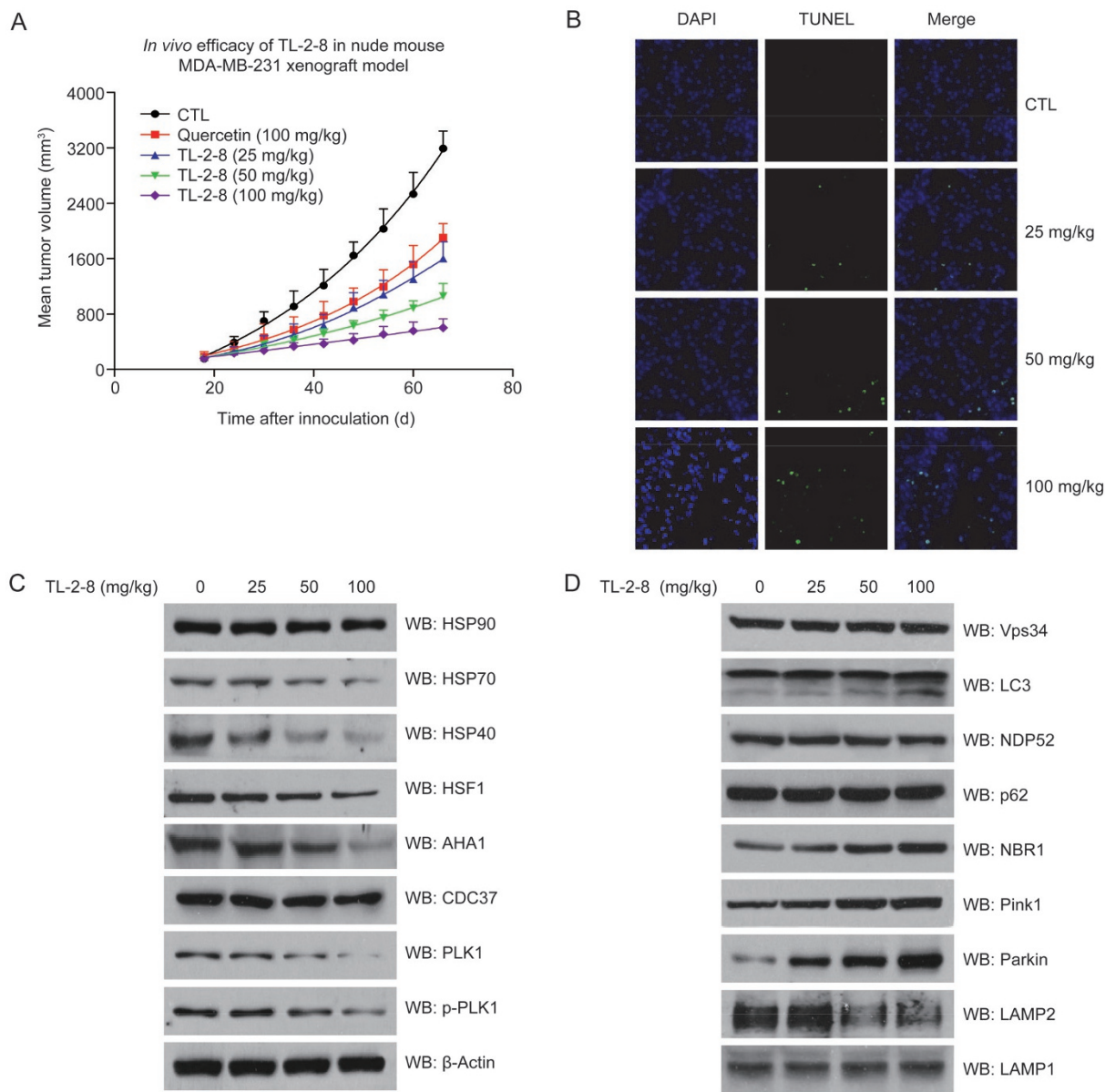


Figure 7. TL-2-8 inhibited tumor growth *in vivo* in MDA-MB-231 cell xenografted mice. (A) Tumor volumes from each treatment group during the study period. (B) Representative images of TUNEL staining in MDA-MB-231 breast cancer tumors in mice treated with control vehicle and TL-2-8. Original magnification: 40 \times . (C) Typical Hsp90 co-chaperones and clients as well as (D) autophagic proteins were detected by Western blotting in tumor samples.

cells, where it is involved in the maturation, activation, and stabilization of its client proteins, which include numerous transcription factors and kinases. Hsp90 performs its chaperone functions with the help of a series of co-chaperones, including AHA1, Cdc37, Hsp70 and Hsp40. In cancer cells, most Hsp90 client proteins play critical roles in cancer cell survival and proliferation. The abrogation of Hsp90 results in the depletion of client proteins involved in tumor cell proliferation, survival, and all of the hallmark traits of malignancy. Thus, Hsp90 is an important target for anti-cancer drug development.

AHA1 is a critical co-chaperone for the Hsp90 protein folding cycle and for the conformational alteration of Hsp90, which facilitates its ATPase activity. Silencing of AHA1 expression decreases Hsp90 client protein activation. Therefore, targeting AHA1 could be an alternative way to develop anti-cancer drugs that interfere with Hsp90 chaperone cycling. In this study, we demonstrated for the first time that TL-2-8 directly abrogates AHA1 expression, thereby decreasing Hsp90/AHA1 complex formation and impeding Hsp90 chaperone function. No undesirable side effects of TL-2-8 treatment were observed, which contrasts with the adverse effects observed upon treatment with 17-AAG, PU-H71 and NVP-AUY922^[26]; Hsp90 inhibitors have a tendency to induce an increase in the mRNA and protein levels of the antiapoptotic chaperones Hsp27, Hsp40 and Hsp70. No such effects were observed upon TL-2-8 treatment, as TL-2-8 directly diminishes Hsp90/AHA-1 complex formation, resulting in the decreased induction of HSPs in response to heat shock through the downregulation of HSF1.

LAMP2, a lysosomal membrane protein, plays an important role in lysosomal stability as well as in autophagy. The overexpression of LAMP2 increases autophagy activity, and this effect is accompanied by decreased levels of p62 and enhanced expression of LC3. By contrast, LAMP2-knockout animals accumulate autophagic vacuoles, and this leads to the blockade of autophagy and to p62 protein accumulation in mice^[24]. The heat shock proteins Hsp70 and Hsp90 exist as part of the chaperone complex that is associated with the lysosomal membrane^[27]. The interaction of LAMP2 with Hsp90 is critical for preserving the stability of LAMP2 at the lysosomal membrane and for the functional dynamics of LAMP2 complexes.

Similarly to the effect of Hsp90 inhibitors^[28], TL-2-8 reduced the total levels of LAMP2, indicating a possible decreased stability of the LAMP2 protein in lysosomes. As lysosomal membrane-associated Hsp90, but not cytosolic Hsp90, has a stabilizing effect on LAMP2, the TL-2-8-induced decrease in LAMP2 levels may be due to the disruption of the association of the Hsp90/AHA1 complex with the luminal side of the lysosomal membrane. Lysosomes are the terminal degradative compartment for autophagy, and LAMP2 plays a critical role in the fusion of autophagosomes with lysosomes, which forms autolysosomes. The forced overexpression of LAMP2 increases the fusion of lysosomes and autophagosomes, leading to increased autophagy activity and decreased p62 expression in MDA-MB-231 cells stably expressing Flag-LAMP2 (Fig-

ures 6C and 6D). As expected, in MDA-MB-231-xenografted mice, TL-2-8 treatment increased the expression levels of NBR1 but decreased the LAMP2 levels, indicating the blockade of autophagosome-lysosome fusion through TL-2-8-mediated depletion of LAMP2 (Figure 7D).

As a novel inhibitor of AHA1, TL-2-8 downregulated the chaperone function of Hsp90, leading to the degradation of kinase client proteins in MDA-MB-231 and MDA-MB-468 breast cancer cells. Most Hsp90 kinase clients are crucial for tumorigenesis. We found that AHA1 inhibition by TL-2-8 decreased the phosphorylation of the key signaling protein PLK1, resulting in the inactivation of downstream signaling pathways and subsequent cellular processes. The downregulation of PLK1 protein levels in TL-2-8-treated breast cancer cells was strongly correlated with the inhibition of Parkin activity during mitophagy maturation. Consequently, TL-2-8 is specifically effective at killing cancer cells *in vitro* and *in vivo*.

Even though the precise anti-cancer mechanism of the flavonoid TL-2-8 remains to be fully elucidated, our findings highlight that TL-2-8 inhibits tumor development by serving as an AHA1 inhibitor. The efficacy of TL-2-8 in suppressing cancer cell growth *in vitro* and *in vivo* suggests its potential use in cancer therapy, especially because it is associated with fewer adverse effects than are other Hsp90 inhibitors.

Acknowledgements

We are grateful to the facility Core Platform for the flow cytometry analysis and cell imaging at the School of Pharmacy, Fudan University. This work was supported by grants from the National Natural Science Foundation of China (grant numbers 81272391 and 81572721 to Yong-hua YANG).

Author contribution

Hui-juan LIU, Xiao-xiao JIANG, Yi-zhen GUO, Fang-hui SUN, Xin-hui KOU, Yong BAO, Zhu-qing ZHANG, Zhao-hu LIN, and Ting-bo DING performed the experiments; Hui-juan LIU, Lan JIANG and Yong-hua YANG analyzed the data and designed the experiments; Xin-sheng LEI synthesized the compound TL-2-8; Yong-hua YANG provided supervision and wrote the manuscript.

Supplementary information

Supplementary information is available on the website of *Acta Pharmacologica Sinica*.

References

- 1 Benavente-Garcia O, Castillo J. Update on uses and properties of citrus flavonoids: new findings in anticancer, cardiovascular, and anti-inflammatory activity. *J Agric Food Chem* 2008; 56: 6185–205.
- 2 Murakami A, Ashida H, Terao J. Multitargeted cancer prevention by quercetin. *Cancer Lett* 2008; 269: 315–25.
- 3 Sak K. Site-specific anticancer effects of dietary flavonoid quercetin. *Nutr Cancer* 2014; 66: 177–93.
- 4 Brito AF, Ribeiro M, Abrantes AM, Pires AS, Teixo RJ, Tralhao JG, et al. Quercetin in cancer treatment, alone or in combination with conventional therapeutics? *Curr Med Chem* 2015; 22: 3025–39.

- 5 Kim JA, Lee S, Kim DE, Kim M, Kwon BM, Han DC. Fisetin, a dietary flavonoid, induces apoptosis of cancer cells by inhibiting HSF1 activity through blocking its binding to the hsp70 promoter. *Carcinogenesis* 2015; 36: 696–706.
- 6 Saito H, Tsujitani S, Oka S, Kondo A, Ikeguchi M, Maeta M, et al. An elevated serum level of transforming growth factor-beta 1 (TGF-beta 1) significantly correlated with lymph node metastasis and poor prognosis in patients with gastric carcinoma. *Anticancer Res* 2000; 20: 4489–93.
- 7 Wei YQ, Zhao X, Kariya Y, Fukata H, Teshigawara K, Uchida A. Induction of apoptosis by quercetin: involvement of heat shock protein. *Cancer Res* 1994; 54: 4952–7.
- 8 Ritossa F. Discovery of the heat shock response. *Cell Stress Chaperones* 1996; 1: 97–8.
- 9 Didelot C, Lanneau D, Brunet M, Joly AL, De Thonel A, Chiosis G, et al. Anti-cancer therapeutic approaches based on intracellular and extracellular heat shock proteins. *Curr Med Chem* 2007; 14: 2839–47.
- 10 Whitesell L, Lindquist SL. HSP90 and the chaperoning of cancer. *Nat Rev Cancer* 2005; 5: 761–72.
- 11 Trepel J, Mollapour M, Giaccone G, Neckers L. Targeting the dynamic HSP90 complex in cancer. *Nat Rev Cancer* 2010; 10: 537–49.
- 12 Yang Y, Rao R, Shen J, Tang Y, Fiskus W, Nechtman J, et al. Role of acetylation and extracellular location of heat shock protein 90alpha in tumor cell invasion. *Cancer Res* 2008; 68: 4833–42.
- 13 Yang Y, Fiskus W, Yong B, Atadja P, Takahashi Y, Pandita TK, et al. Acetylated hsp70 and KAP1-mediated Vps34 SUMOylation is required for autophagosome creation in autophagy. *Proc Natl Acad Sci U S A* 2013; 110: 6841–46.
- 14 Joo JH, Dorsey FC, Joshi A, Hennessy-Walters KM, Rose KL, McCastlain K, et al. Hsp90-Cdc37 chaperone complex regulates Ulk1- and Atg13-mediated mitophagy. *Mol Cell* 2011; 43: 572–85.
- 15 van Erk MJ, Roepman P, van der Lende TR, Stierum RH, Aarts JM, van Bladeren PJ, et al. Integrated assessment by multiple gene expression analysis of quercetin bioactivity on anticancer-related mechanisms in colon cancer cells *in vitro*. *Eur J Nutr* 2005; 44: 143–56.
- 16 Piper PW, Millson SH. Mechanisms of resistance to Hsp90 inhibitor drugs: a complex mosaic emerges. *Pharmaceuticals (Basel)* 2011; 4: 1400–22.
- 17 Holmes JL, Sharp SY, Hobbs S, Workman P. Silencing of HSP90 co-chaperone AHA1 expression decreases client protein activation and increases cellular sensitivity to the HSP90 inhibitor 17-allylamino-17-demethoxygeldanamycin. *Cancer Res* 2008; 68: 1188–97.
- 18 Chen Y, Dorn GN. PINK1-phosphorylated mitofusin 2 is a Parkin receptor for culling damaged mitochondria. *Science* 2013; 340: 471–5.
- 19 Kane LA, Lazarou M, Fogel AI, Li Y, Yamano K, Sarraf SA, et al. PINK1 phosphorylates ubiquitin to activate Parkin E3 ubiquitin ligase activity. *J Cell Biol* 2014; 205: 143–53.
- 20 Ordureau A, Sarraf SA, Duda DM, Heo JM, Jedrychowski MP, Sviderskiy VO, et al. Quantitative proteomics reveal a feedforward mechanism for mitochondrial PARKIN translocation and ubiquitin chain synthesis. *Mol Cell* 2014; 56: 360–75.
- 21 Shiba-Fukushima K, Imai Y, Yoshida S, Ishihama Y, Kanao T, Sato S, et al. PINK1-mediated phosphorylation of the Parkin ubiquitin-like domain primes mitochondrial translocation of Parkin and regulates mitophagy. *Sci Rep* 2012; 2: 1002.
- 22 Lee SB, Kim JJ, Nam HJ, Gao B, Yin P, Qin B, et al. Parkin regulates mitosis and genomic stability through Cdc20/Cdh1. *Mol Cell* 2015; 60: 21–34.
- 23 Levine B, Kroemer G. Autophagy in the pathogenesis of disease. *Cell* 2008; 132: 27–42.
- 24 Tanaka Y, Guhde G, Suter A, Eskelinen EL, Hartmann D, Lullmann-Rauch R, et al. Accumulation of autophagic vacuoles and cardiomyopathy in LAMP-2-deficient mice. *Nature* 2000; 406: 902–6.
- 25 Fortunato F, Burgers H, Bergmann F, Rieger P, Buchler MW, Kroemer G, et al. Impaired autolysosome formation correlates with Lamp-2 depletion: role of apoptosis, autophagy, and necrosis in pancreatitis. *Gastroenterology* 2009; 137: 350–60, 360–61.
- 26 Caldas-Lopes E, Cerchietti L, Ahn JH, Clement CC, Robles AI, Rodina A, et al. Hsp90 inhibitor PU-H71, a multimodal inhibitor of malignancy, induces complete responses in triple-negative breast cancer models. *Proc Natl Acad Sci U S A* 2009; 106: 8368–73.
- 27 Agarraberes FA, Terlecky SR, Dice JF. An intralysosomal hsp70 is required for a selective pathway of lysosomal protein degradation. *J Cell Biol* 1997; 137: 825–34.
- 28 Bandyopadhyay U, Kaushik S, Varticovski L, Cuervo AM. The chaperone-mediated autophagy receptor organizes in dynamic protein complexes at the lysosomal membrane. *Mol Cell Biol* 2008; 28: 5747–63.